Microgonotropens and Their Interactions with DNA. 4.[1] Synthesis of the Tripyrrole Peptides Tren-Microgonotropen-a and -b and Characterization of Their Interactions with dsDNA

Gong-Xin He, Kenneth A. Browne, Andrei Blaskó, and Thomas C. Bruice*

Contribution from the Department of Chemistry, University of California at Santa Barbara, Santa Barbara, California 93106

*Received October 27, 1993**

Abstract: The novel concept of attaching a connector to a pyrrole nitrogen of a tripyrrole peptide minor groove binding agent to carry functionalities to the phosphates and major groove of DNA has been extended with the synthesis of tren-microgonotropen-a and -b {**6a** and **6b**; Chart 1}. The tren-microgonotropens are tripeptides of 3-aminopyrrole-2-carboxylic acid where (i) the amino terminus is acetylated; (ii) the terminal carboxyl has an amide linkage to β-(*N*,*N*-dimethylamino)propylamine; (iii) the ring nitrogens of the first and third pyrrole rings are *N*-methylated; and (iv) the ring nitrogen of the central pyrrole carries the substituents $-(CH_2)_3NH(CH_2)_2N\{(CH_2)_2NH_2\}_2$ (**6a**) and $-(CH_2)_4NH(CH_2)_2N\{(CH_2)_2NH_2\}_2$ (**6b**). To determine the sequence specificity of binding, complementary strand analysis by DNase I footprinting of **6a**,**b** bound to the 5′- and 3′-[^{32}P] labeled 167 bp *Eco*RI/*Rsa*I restriction fragment of pBR322 was carried out. Results show clear and specific cleavage inhibition patterns at three of the four potential A + T-rich binding sites. Employing Hoechst 33258 (**Ht**) as a fluorescent titrant, the equilibrium constants for the binding of **6a**,**b** to the hexadecameric duplex d(GGCGCAAATTTGGCGG)/d(CCGCCAAATTTGCGCC) were determined (35 °C). The equilibrium constants for the formation of 1:1 (K_{L1}) and 2:1 (K_{L2}) complexes with **6a**,**b** and **5a**–**c** (the dien-microgonotropens) exhibit a slight degree of cooperativity {$K_{L2} > K_{L1}$}. The product $K_{L1}K_{L2}$ was slightly greater for **6a** and **6b** than for the dien-microgonotropens **5a**, **5b**, and **5c**. In addition, we now show that **Ht** forms a 1:1 and a 2:1 complex with the hexadecamer not only by fluorescence titration but also by ^{1}H NMR titrations. The electrophoretic mobilities of φX-174-RF DNA *Hae*III restriction fragments complexed to **6a** or **6b** revealed a much greater conformational change in the DNA fragments than when distamycin (**Dm**) was bound to the same fragments and about a 2-fold greater change than generated by the dien-microgonotropens. Complete inhibition of mammalian topoisomerase I with 30 μM **6b** was observed while dien-microgonotropen-b and **Dm** only partially inhibited topoisomerase I at 150 μM. Thus, evidence from equilibrium constants for complexation, electrophoretic mobilities, and topoisomerase I assays suggests that **6b** alters the conformation of DNA in a manner that is not directly related to the affinity of complexation.

Introduction

Interest in reagents capable of sequence selective nonintercalative complexation to DNA, particularly small organic compounds able to complex to the minor groove of B-DNA, has drawn considerable attention in recent years. A crescent shape to match the natural curvature of the minor groove of B-DNA is a common feature of each of these molecules.[7] New among the minor groove binding molecules are the microgonotropens[2,4] in which the *N*-methyl substituent of **2**'s (Chart 1) central pyrrole moiety is replaced with linkers of varying chain length that may terminate in recognition or "warhead" moieties. The microgonotropens (Chart 1) are capable of binding the minor groove of DNA sequence selectively, reaching up and out of the minor groove with their polyamine moieties, and firmly grasping the phosphodiester backbone. In so doing, the microgonotropens are able to increase their binding affinities to DNA and alter the conformation of DNA.

We report here the synthesis of the tren-microgonotropens **6a** and **6b**, the characterization of their binding to dsDNA (selectivity of sequence and equilibrium binding constants), and the electrophoretic mobility of DNA complexed by **6a** and **6b** as well as the latter's inhibition of calf thymus topoisomerase I's ability to unwind supercoiled DNA. The ability to alter the conformation of DNA with small organic molecules at selected sites may have profound consequences on influencing DNA modifying enzymes and on controlling regulation of genetic expression.

Results and Discussion

Synthesis. Our synthesis of **6a**,**b** (Schemes 1 and 2) began with the preparation of the central pyrrole units (**8a**,**b**) in which the tren group was attached to the pyrrole through the desired linker arms. Attempts at purification of **8a**,**b** through column chromatography failed. Very poor separation was obtained over an Al_2O_3 column. In addition, use of a SiO_2 column led to the hydrolysis of the ester group in **8**. Compound **8** (5%) was obtained only as a mixture of the methyl ester (5%) and the carboxylate (20%) with SiO_2 column chromatography by elution with MeOH: concentrated NH_3 (aqueous) = 80:20. It seems that the polyamino group can complex trace amounts of metal ion from the SiO_2 which consequently catalyzes the hydrolysis of the ester group. Due to these complexities in attempted purification, crude **8**, which by ^{1}H NMR showed only ~5% impurity, was used in the next reaction without purification.

Attempts to employ *tert*-butyl *S*-4,6-dimethylpyrimid-2-yl thiocarbonate as an agent to deliver the *tert*-butyl carbamate[8] (Boc) as a protecting group for the primary and secondary amines

* Abstract published in *Advance ACS Abstracts*, April 1, 1994.

(1) (a) Part 6 of the series Chemistry of Phosphodiesters, DNA and Models. References 2–6 are previous publications in this series. (b) Microgonotropens are defined as DNA minor groove binding agents with substituents which project outward from the minor groove and terminate with either interactions with the phosphodiester backbone or with interactions in the major groove. A prefix denotes the nature of the projecting substituent (in this study, tren-microgonotropens). Suffixes (-a, -b, etc.) are used to differentiate among related analogues (i.e., that vary by methylene linker chain length).

(2) Bruice, T. C.; Mei, H.-Y.; He, G.-X.; Lopez, V. *Proc. Natl. Acad. Sci. U.S.A.* **1992**, *89*, 1700.

(3) Browne, K. A.; Bruice, T. C. *J. Am. Chem. Soc.* **1992**, *114*, 4951.

(4) He, G.-X.; Browne, K. A.; Groppe, J. C.; Blaskó, A.; Mei, H.-Y.; Bruice, T. C. *J. Am. Chem. Soc.* **1993**, *115*, 7061.

0002-7863/94/1516-3716$04.50/0

Chart 1

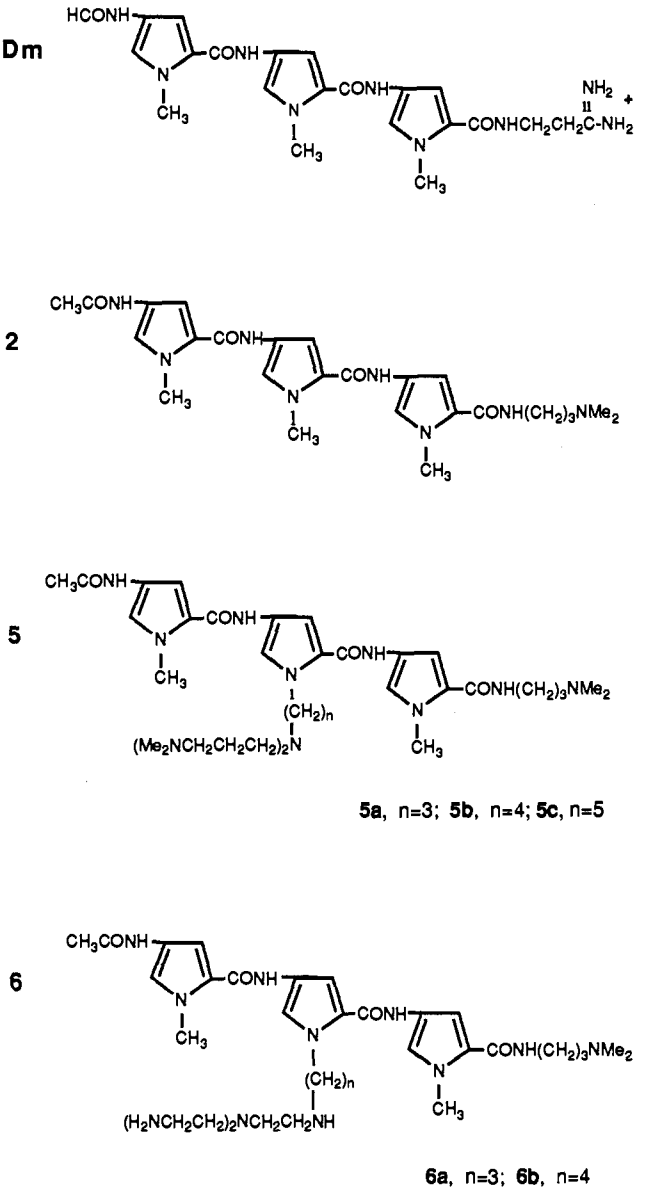

Scheme 1

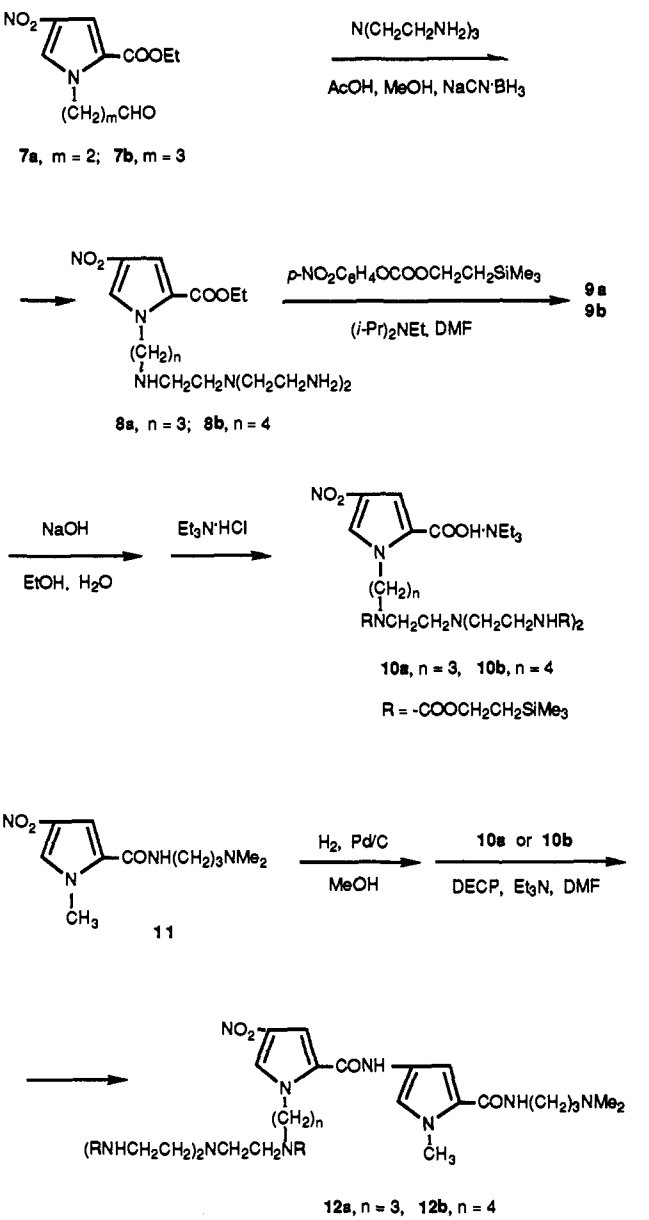

of **8** provided but ~30% yields of product. Changing the synthetic methodology by using 2-trimethylsilylethyl carbamate[9] (Teoc) for the protection of the tren polyamino group on **8** provided **9** in a 52–61% yield after separation by SiO_2 column chromatography (Schemes 1 and 2). Additional factors in favor of the choice of this protecting group included its stability toward the conditions of hydrogenation over Pd/C and other harsh conditions employed in the synthetic steps. Compound **6**, like **8**, was difficult to purify since it did not migrate on SiO_2 TLC even with the elution solvent mixture of MeOH:concentrated NH_3 (aqueous) = 60:40. Fortunately, the deprotection reaction of **14** (acid catalyzed removal of the Teoc group with CF_3COOH) produces only the desired product and volatile compounds.[9] ^1H NMR indicated that subsequent treatment of the crude **6** product with HO^- exchange resin gave very pure **6**.

DNase I Footprint Analysis of 6a and 6b. DNase I was employed as the DNA cleaving agent for footprint generation[10] in the comparative analysis of the interactions of **6a**, **6b**, and distamycin with the 167 bp *Eco*RI/*Rsa*I pBR322 restriction fragment. Four A + T-rich binding sites for distamycin,[11] bromoacetyldistamycin,[12] and the dien-microgonotropens[4] have been previously identified {bold typeface, Figure 1}, making this an ideal DNA fragment for the comparative study of the tren-microgonotropens with distamycin. DNase I has an advantage over Tullius' HO•[13] and Dervan's **MPE**·Fe(II)[14] in that it cleaves

(5) Browne, K. A.; He, G.-X.; Bruice, T. C. *J. Am. Chem. Soc.* **1993**, *115*, 7072.
(6) Blaskó, A.; Browne, K. A.; He, G.-X.; Bruice, T. C. *J. Am. Chem. Soc.* **1993**, *115*, 7080.
(7) (a) Kopka, M. L.; Yoon, C.; Goodsell, D.; Pjura, P.; Dickerson, R. E. *Proc. Natl. Acad. Sci. U.S.A.* **1985**, *82*, 1376. (b) Coll, M.; Frederick, C. A.; Wang, A. H.-J.; Rich, A. *Proc. Natl. Acad. Sci. U.S.A.* **1987**, *84*, 8385. (c) Teng, M.-K.; Usman, N.; Frederick, C. A.; Wang, A. H.-J. *Nucleic Acids Res.* **1988**, *16*, 2671. (d) Carrondo, M. A. A. F. de C. T.; Coll, M.; Aymami, J.; Wang, A. H.-J.; van der Marel, G. A.; van Boom, J. H.; Rich, A. *Biochemistry* **1989**, *28*, 7849. (e) Scahill, T. A.; Jensen, R. M.; Swenson, D. H.; Hatzenbuhler, N. T.; Petzold, G. L.; Wierenga, W.; Brahme, N. M. *Biochemistry* **1990**, *29*, 2852. (f) Chen, S.-M.; Leupin, W.; Rance, M.; Chazin, W. J. *Biochemistry* **1992**, *31*, 4406. (g) Edwards, K. J.; Jenkins, T. C.; Neidle, S. *Biochemistry* **1992**, *31*, 7104.
(8) Nagasawa, T.; Kuroiwa, K.; Narita, K.; Isowa, Y. *Bull. Chem. Soc. Jpn.* **1973**, *46*, 1269.
(9) (a) Carpino, L. A.; Tsao, J.-H. *J. Chem. Soc., Chem. Commun.* **1978**, 358. (b) Rosowsky, A.; Wright, J. E. *J. Org. Chem.* **1989**, *54*, 5551.
(10) Galas, D. J.; Schmitz, A. *Nucleic Acids Res.* **1978**, *5*, 3157.
(11) Harshman, K. D.; Dervan, P. B. *Nucleic Acids Res.* **1985**, *13*, 4825.
(12) Baker, B. F.; Dervan, P. B. *J. Am. Chem. Soc.* **1989**, *111*, 2700.
(13) Burkhoff, A. M.; Tullius, T. D. *Cell* **1987**, *48*, 935.
(14) Van Dyke, M. W.; Hertzberg, R. P.; Dervan, P. B. *Proc. Natl. Acad. Sci. U.S.A.* **1982**, *79*, 5470.

Scheme 2

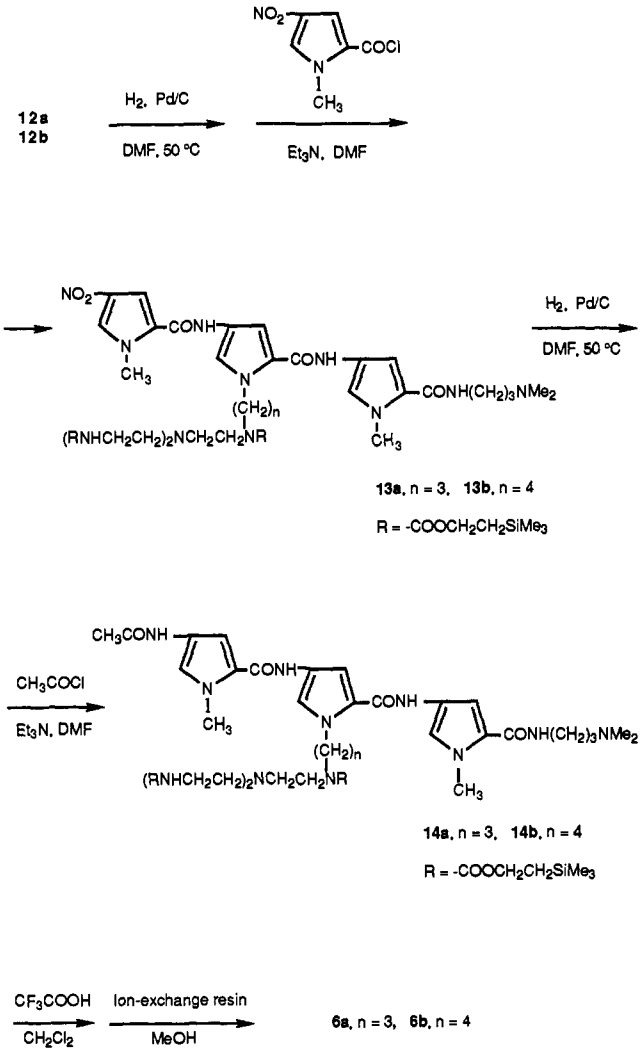

precisely at the 5′ edge of an agent's minor groove binding site, producing a protected region with a sharp, well-defined 5′ border.[15] Thus, even though DNase I cleavage at the 3′ edge of the binding site is not precisely defined, complementary strand analysis provides sharply defined 5′ borders on both DNA strands {Figure 1}, and, hence, precisely defined binding sites that correspond closely to those previously defined.[4]

DNase I footprinting analysis of the 3′-[^{32}P] labeled 167 bp *Eco*RI/*Rsa*I restriction fragment with **6a** and **6b** {Figure 2b}, when coupled with results from the 5′-labeled material {Figure 2a}, defined binding sites similar to those for distamycin. Preincubation of the 167 bp 3′- and 5′-[^{32}P] labeled restriction fragments with 5 μM **6a**, **6b**, or distamycin (0.05 ligand/bp DNA) did not produce detectable inhibition of DNase I cleavage at any of the four A + T-rich binding sites {Figure 2}. In contrast, specific inhibition of cleavage was observed at three of the four sites (sites II, III, IV) after preincubation with 25 and 50 μM **6a**, **6b**, or distamycin (0.25 and 0.5 ligand/bp DNA). Site I could only be distinguished at 100 μM, and, even then, site definition was vague. Preincubation of the restriction fragment with 100 μM ligand (1.0 ligand/bp DNA) resulted in additional protection from DNase I cleavage within the spacer regions which flank the A + T-rich binding sites. Dervan and co-workers have observed a similar binding isotherm for distamycin on the 516 bp *Rsa*I/*Eco*RI restriction fragment of pBR332. At higher concentrations

Figure 1. Partial nucleotide sequence of the 167 bp *Eco*RI/*Rsa*I restriction fragment from plasmid pBR322 detailing four A + T-rich binding sites (bold type). The oligonucleotide primer for synthesis of dideoxynucleotide sequencing products is depicted by a horizontal arrow adjacent the annealing site. Positions of incorporated radiolabel in the oligonucleotide primer, 5′-labeled strand, and 3′-labeled strand are indicated with asterisks. Vertical arrows depict cleavages proximal to the protected sites. These were determined by the analysis of both 5′ (downward arrows) and 3′ (upward arrows) labeled restriction fragments at a binding agent concentration of 50 μM.

of distamycin (3.1 ligand/bp DNA), spacer regions which flanked A + T-rich binding sites coalesced into a single, broad, protected zone.[14]

Analysis of the 5′ footprint edges of the binding sites of 50 μM **6a**, **6b**, and distamycin shows cleavage patterns that are very similar to those seen previously for the dien-microgonotropens.[4] Closer scutiny reveals small changes for sites II and III, while site IV is unchanged. Site III is one base smaller on the 3′ strand, and site II is two bases smaller on the 3′ strand than was found for the dien-microgonotropens[4] {Figure 1}. Even at the highest concentrations of **6a** and **6b**, enhancements in or increased rates of DNase I cleavage were not observed at specific sequences for the 5′- and the 3′-[^{32}P] labeled restriction fragments (**Dm** showed enhancements similar to those found previously).[4]

Hoechst 33258 Associations with Single A + T-Rich DNA Binding Sites. Hoechst 33258 (**Ht**) is a synthetic dye that becomes highly fluorescent upon binding the minor groove of A + T-rich dsDNA.[16] This property makes **Ht** an excellent molecule to study in associations with duplex DNA under *ideal* conditions (5×10^{-9} M) by fluorescence spectroscopy. We have previously shown by titrations in which an increase in fluorescence was observed with increasing concentrations of **Ht** that a single A_3T_3 DNA oligomer binding site {d(GGCGCAAATTTGGCGG)/d(CCGCCAAATTTGCGCC)} can accommodate not just one, but two molecules of **Ht** in the stepwise manner outlined in Scheme 3.[5] This had *not* been shown previously. We have now substantiated this finding by following the titration of dodecameric and hexadecameric dsDNA with **Ht** by ^{1}H NMR spectroscopy.

Titrations of DNA Oligomers with Hoechst 33258 Utilizing ^{1}H NMR. ^{1}H NMR titrations of solutions containing 3.8×10^{-4} M of either d(CGCAAATTTGCG)$_2$ {Figure 3a; μ = 0.12} or d(GGCGCAAATTTGGCGG)/d(CCGCCAAATTTGCGCC) {Figure 4a; μ = 0.20} with Hoechst 33258 (**Ht**) were carried out in D_2O at 21 °C in 0.25 mol equivalent steps (0.01 M potassium phosphate, pH 7.0, 0.01 M NaCl) in the presence of 2,4,6-trimethyl benzoate (mesitoate, 3.8×10^{-4} M) as an internal standard. The effects of the titration were followed by observing the disappearance of the overlapped thymidine CH_3 resonances at 1.60–1.70 ppm {Figures 3a and 4a; marked with an *} and the appearance of new nonequivalent thymidine CH_3 resonances at 1.35–1.45 ppm. The titration can also be monitored by the appearance of a new set of adenosine H8 resonances downfield from the uncomplexed oligomer. Spectral changes occur up to a 2.0 mol ratio of **Ht**/oligomer. The existence of nonequivalent N-CH_3's upon reaching the 2:1 mol ratios of **Ht**/hexadecamer {Figure 4a} shows that the 2:1 binding mode is not

(15) (a) Dabrowiak, J. C.; Goodisman, J. In *Chemistry & Physics of DNA–Ligand Interactions*; Kallenbach, N. R., Ed.; Adenine Press: New York, 1989; pp 143–174. (b) Goodisman, J.; Dabrowiak, J. C. *Biochemistry* **1992**, *31*, 1058.

(16) Loontiens, F. G.; Regenfuss, P.; Zechel, A.; Dumortier, L.; Clegg, R. M. *Biochemistry* **1990**, *29*, 9029.

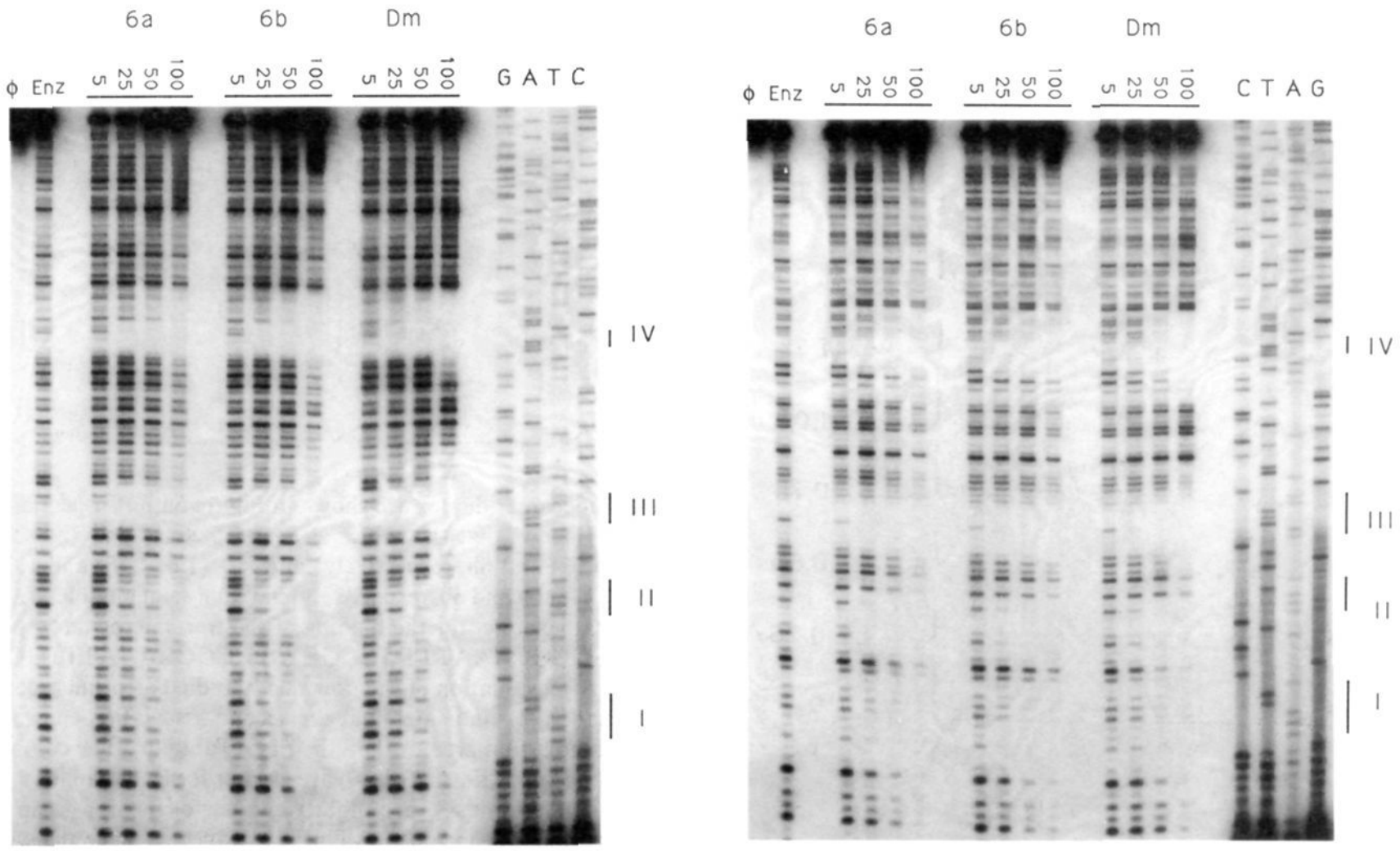

Figure 2. DNase I footprint analysis of the binding of the tren-microgonotropens and distamycin (**Dm**) to (a, left) the 5′-labeled 167 bp *Eco*RI/*Rsa*I restriction fragment and (b, right) the 3′-labeled 167 bp *Eco*RI/*Rsa*I restriction fragment. In lane 1, ϕ indicates intact DNA; lane 2, Enz is the abbreviation for DNase I cleavage of unprotected DNA; lanes 3–14, DNase I footprinting reactions containing **6a**, **6b**, and **Dm**, respectively, are at the concentrations indicated in μM. Products of the four dideoxynucleotide sequencing reactions (GATC) were synthesized by extension of the 5′-labeled oligonucleotide primer depicted to Figure 1. The same sequencing reactions were used for the 3′ sequence ladder by exchanging the complementary base pairs (G with C; C with G; A with T; T with A). The four A + T-rich binding sites depicted in Figure 1 are indicated adjacent to the DNA sequence ladder.

Scheme 3

$$\text{DNA} \underset{}{\overset{K_{Ht1}[\mathbf{Ht}]}{\rightleftharpoons}} \text{DNA:}\mathbf{Ht} \underset{}{\overset{K_{Ht2}[\mathbf{Ht}]}{\rightleftharpoons}} \text{DNA:}\mathbf{Ht}_2$$

symmetric; this is as expected due to the asymmetric nature of the hexadecamer sequence. The *N*-CH_3 resonances of the piperazine ring of **Ht** can be seen forming at 3.00 ppm in the case of the dodecamer and at 2.98 and 3.00 ppm in the case of the hexadecamer (2.78 ppm for **Ht** alone in the same conditions) and increases up to 2.0 **Ht**/oligomer {Figure 3a and 4a}. The *ortho* CH_3 resonances (2.23 ppm; 6H) of the internal standard {[mesitoate] = [dodecamer]} were used in order to check the stoichiometry of binding. The methyl protons of mesitoate integrate 1:1 with the two equivalent *N*-CH_3's of **Ht** when complexed to the symmetric dodecamer {Figure 3b} and also 1:1 with the nonequivalent *N*-CH_3's of **Ht** when complexed with the pseudosymmetric hexadecamer {Figure 4b}. In addition they integrate 1:1 with each of the three thymidine CH_3's of the nonequivalent (+) and (–) strands of the oligomers {Figures 3c and 4c}. The ^{1}H NMR titration of 4.0×10^{-4} M hexadecamer in H_2O (10% D_2O) with **Ht** allowed perturbations in the imino region (12.5–14.2 ppm) of the DNA to be followed {Figure 4d}. The spectrum changed up through a 2:1 **Ht**/hexadecamer ratio and then remained unchanged at greater **Ht** concentrations (2.5:1 **Ht**/hexadecamer). The binding is asymmetric with an increase in the number of A + T imino resonances from 6 (free hexadecamer) to 12 (free + complexed hexadecamer) and then back down to 6 (complexed hexadecamer), confirming the results in D_2O. As was found in the case of distamycin,[17] the binding is not perturbed by the existence of mesitoate nor by the temperature increase from 21 to 35 °C.

(17) Blaskó, A.; Bruice, T. C. *Proc. Natl. Acad. Sci. U.S.A.* **1993**, *90*, 10018.

Equilibrium constants for the association of 6a and 6b with oligomeric DNA were assessed by the complexing of tren-microgonotropen-a and -b to the hexadecamer d(GGCG-CAAATTTGGCGG)/d(CCGCCAAATTTGCGCC) in aqueous solutions at 35 °C (2.8 mL solutions containing 0.01 M phosphate buffer, pH 7.0, and 0.01 M NaCl). These reactions were followed by the competition of the dye Hoechst 33258 (**Ht**) with **6a** and **6b** for the A_3T_3 minor groove binding site (an extention of **Ht** alone binding to dsDNA). The concentrations of **6a** and **6b** were confirmed by ^{1}H NMR peak integration of resonances with those of an equivalent concentration of mesitoate. As shown previously,[5] monitoring the increase in fluorescence intensity as the association of **Ht** with the hexadecamer displaces prebound nonfluorescent ligands is an excellent method for determining equilibrium binding constants. Scheme 4 relates the equilibrium constants for the complexing of one and two **Ht** species to the hexadecamer with one and two **L** (where **L** = **6a** or **6b**) binding to the hexadecamer, plus equilibrium constants for the simultaneous binding of one **Ht** and one **L** at the same site. Equation 1, derived from Scheme 4,

$$F = \{\Sigma\Phi K_{Ht1}[\mathbf{Ht}]\ (0.5 + K_{Ht2}[\mathbf{Ht}] + 0.5K_{HtL}[\mathbf{L}]Q')\}/ \{1 + K_{Ht1}[\mathbf{Ht}] + K_{Ht1}K_{Ht2}[\mathbf{Ht}]^2 + K_{Ht1}K_{HtL}[\mathbf{Ht}][\mathbf{L}] + K_{L1}[\mathbf{L}] + K_{L1}K_{L2}[\mathbf{L}]^2\} \quad (1)$$

relates each of the equilibrium binding constants, the total fluorescence ($\Sigma\Phi$), and [**L**] in terms of fluorescence (F) and [**Ht**]. The rationale behind Scheme 4 and the subsequent derivation of eq 1 have been described in considerable detail.[5] The values of $\log K_{Ht1} = 7.6$ and $\log K_{Ht2} = 9.1$ used in this study were determined from a reevaluation of data collected in the previous study[5] and are very close to the previously determined values. A concentration independent static quenching term, Q', is included in eq 1

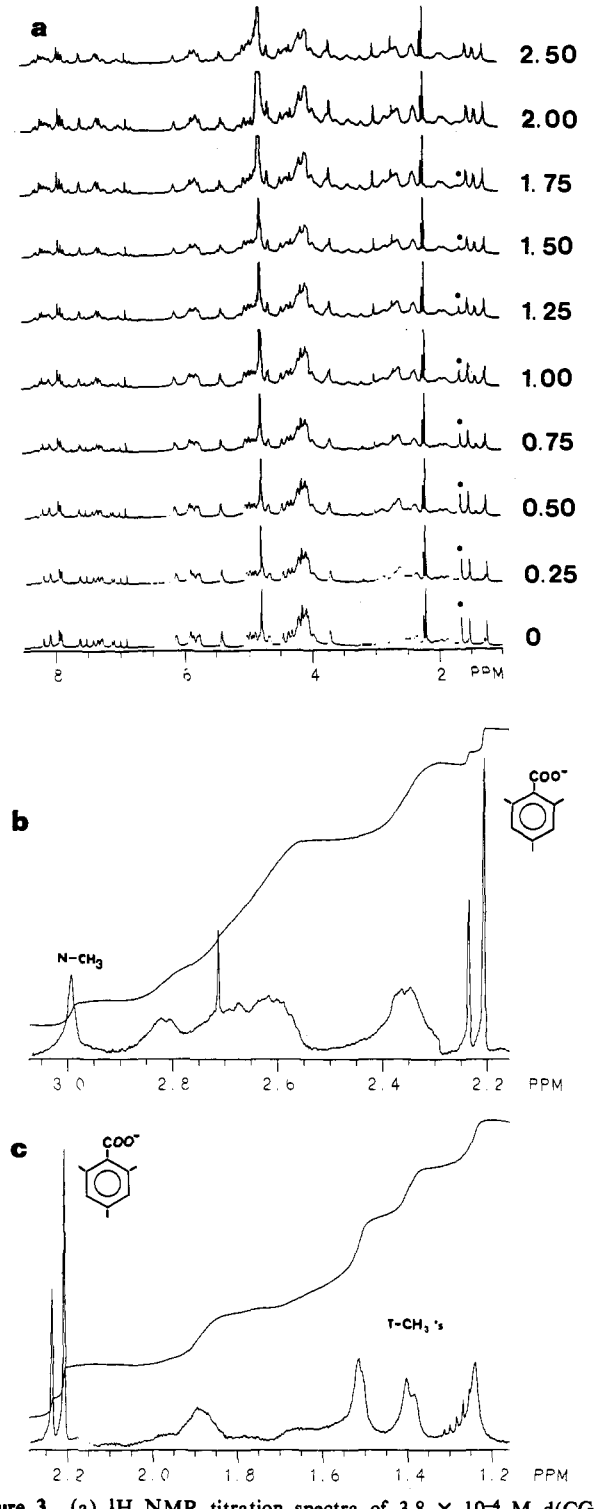

Figure 3. (a) ^{1}H NMR titration spectra of 3.8×10^{-4} M d(CGCAAATTTGCG)$_2$ (0.01 M phosphate buffer, pH 7.0, 0.01 M NaCl, 3.8×10^{-4} M mesitoate) with Hoechst 33258 (Ht) at 21 °C in 0.4 mL of D_2O at the indicated mole ratios of Ht/dodecamer. (b) ^{1}H NMR spectrum at the 2:1 mole ratio of Ht/dodecamer (35 °C) showing that the *ortho* CH_3's (6H) of mesitoate ([mesitoate] = [dodecamer]) at 2.22 ppm integrate 1:1 with the *N*-CH_3 protons of Ht (3.00 ppm) and also 1:1 (c) with each of methyls of the three thymidines (1.2–1.6 ppm) of the (+) and (–) nonequivalent strands.

to account for the lessened fluorescent emission of the DNA:Ht:L complex compared to the DNA:Ht and DNA:Ht$_2$ complexes.

The equilibrium association constants calculated as best fits to the experimental data points for **6a** and **6b** with eq 1 are presented in Table 1. Plots of F vs [Ht] using these constants at 8.0×10^{-9}, 1.0×10^{-8}, 1.2×10^{-8} M ligand and 5.0×10^{-9} M

Scheme 4

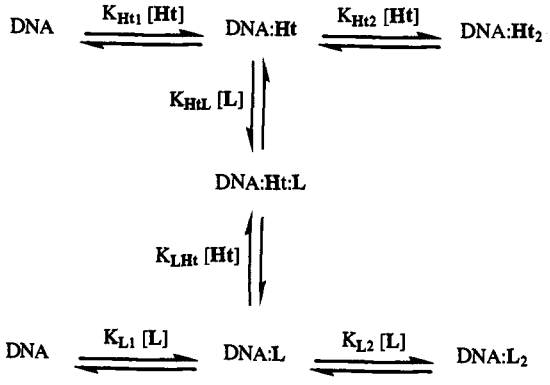

in hexadecamer duplex are shown in Figure 5a,b. Inspection of Table 1 shows that the values of K_{L1} (1.6×10^9 and 7.9×10^8 M^{-1} for **6a** and **6b**, respectively) and K_{L2} (1.6×10^9 and 1.0×10^9 M^{-1} for **6a** and **6b**, respectively) have only a negligible, if any, cooperative effect for the binding of the tren-microgonotropens to d(GGCGCAAATTTGGCGG)/d(CCGCCAAATTTGCGCC). A reevaluation of the previously studied dien-microgonotropens (**5a–c**)[5] indicates that the second association constants are 2.5- to 3-fold greater than the first (Table 1). The complex association constants ($K_{L1}K_{L2}$) are greater for **6a,b** than for **5a–c** since both K_{L1} and K_{L2} are slightly greater for the tren- than for the dien-microgonotropens. This is as expected since there are four amines (including two primary amines) in the tren moiety verses three tertiary amines in the dien group. Primary amines have a higher pK_a than tertiary amines[18] and, therefore, are more prone to hydrogen bond to phosphate linkages. In addition, there is little difference in the association constants of the different microgonotropens within a given series (tren or dien) even though the chain lengths of the linkers differ. This is likely due to the fact that binding ability is a function of both the minor groove binder and the polyamine, with all chain lengths being long enough to permit efficient electrostatic grasping of the phosphodiester backbone.

The degree of fluorescence quenching of Ht in the DNA:Ht:L complexes when L = **6a** and **6b** was also found to be different than for the dien-microgonotropens, while the mode of quenching (intracomplex) was the same for both sets of microgonotropens. From values of Q′ = 0.41 and 0.64 for **6a** and **6b**, respectively, quenching of Ht fluorescence was determined to be 59% and 36%. In contrast, all three of the dien-microgonotropens quenched fluorescence to a constant degree (ca. 45%). Only a small difference in the quenching terms within a given series (tren or dien) would be expected since a given series has a common polyamine. But, in fact, the fluorescence quenching that **6a** causes is considerably more efficient and that of **6b** is somewhat less efficient than that of the dien-microgonotropens. This difference in quenching is likely to be due to special positions that the methylene linkers of **6a** and **6b** confer upon their tren moieities such that the quenching amino groups are in greater or lesser intimate contact with the Ht fluorochrome than is the case with **5a–c**. The fluorescence of solutions containing (i) the hexadecameric DNA duplex plus Ht in the ratio of 1:2 or (ii) the hexadecameric DNA duplex, Ht, and **6b** in the ratio of 1:1:1 did not change on titration with a solution of tris(2-aminoethyl)-amine (data not shown). Thus, as for the dien-microgonotropens,[5] amine quenching is not bimolecular but, rather, by intracomplex quenching within the DNA:Ht:L complex.

Electrophoretic Mobility Shift Assay for 6a and 6b. The effect of the binding of **6a** and **6b** to DNA on the electrophoretic migration has been investigated with ϕX-174-RF DNA *Hae*III restriction digest fragments {Figure 6}. Our use of ϕX-174-RF

(18) Perrin, D. D. *Dissociation Constants of Organic Bases in Aqueous Solution*; Butterworths: London, 1965.

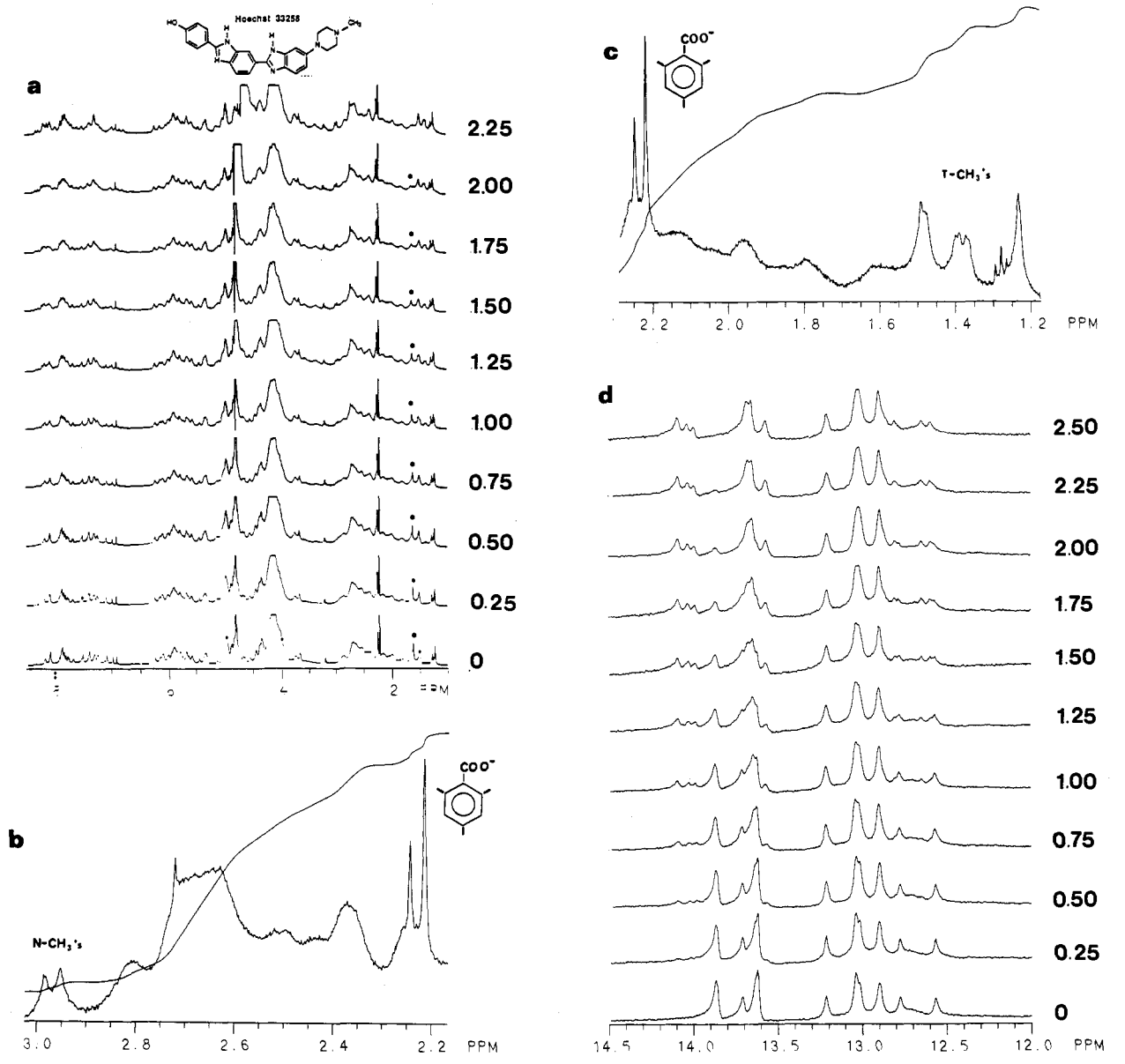

Figure 4. (a) ^{1}H NMR titration spectra of 3.8×10^{-4} M d(GGCGCAAATTTGGCGG)/d(CCGCCAAATTTGCGCC) with **Ht** (0.01 M phosphate buffer, pH 7.0, 0.01 M NaCl, 3.8×10^{-4} M mesitoate) in 0.4 mL of D_2O at 21 °C. (b and c) The ^{1}H NMR spectrum at the 2:1 mole ratio (35 °C) of Ht/hexadecamer. The *ortho* CH_3's (6H) of mesitoate ([mesitoate] = [hexadecamer]) at 2.22 ppm integrate 1:1 with the two *N*-CH_3 protons of the asymmetrically bound Ht (b; 2.98–3.00 ppm) and also 1:1 with each of the three thymidines' methyls of the (+) and (–) strands (c; 1.2–1.6 ppm). (d) ^{1}H NMR titration spectra of 4.0×10^{-4} M hexadecamer (0.01 M phosphate buffer, pH 7.0, 0.01 M NaCl) with **Ht** at 21 °C in 9:1 H_2O:D_2O at the indicated mole ratios of Ht/hexadecamer.

DNA restriction digests in electrophoretic mobility shift assays[4] is predicated on the common use of this material as molecular weight size standards. We have calculated[4] 246 A-tracts (AAAA, AAAT, or TAAA; independent or overlapping) approximately evenly spaced throughout the restriction digest fragments. These are the most preferred binding sites for **6a** and **6b** (*loc. cit.*). When increasing the concentrations of **6a** and **6b** from 20 to 40, 60, and 80 μM (0.088 to 0.176, 0.264, and 0.352 ligand/bp, respectively), the mobility of DNA restriction fragments decreases. Moreover, the decreases in the otherwise approximately logarithmic mobility of the DNA fragments are proportional to their lengths (largest effect seen with the largest fragments). This suggests that the conformation of the DNA is altered significantly by the binding of the tren-microgonotropens, especially in the largest fragments (1358, 1078, and 872 bp).[19] An alternative explanation of the decreased mobility that must be considered is a change in the charge to mass ratio of the DNA: ligand complex. This is unlikely, however, since the shortest fragments do not show the greatest change in mobility as dictated by the logarithmic nature of DNA fragments in an electric field on an agarose gel. Meanwhile, a "smearing" of the bands is evident in the intermediate fragments (603, 310, 281/271, 234, and 194 bp), especially at 60 and 80 μM tren-microgonotropen. This indicates not simply a conformational change but a population of differing conformations of DNA:tren-microgonotropen complexes leading to a distribution of apparent electrophoretic molecular weights. Distamycin brings about smaller changes at 150 μM (0.66 ligand/bp) than **6a** or **6b** at 40 μM. Tris(2-aminoethyl)amine, the tren moiety of the tren-microgonotropens, produces no apparent change in electrophoretic behavior at 150 μM compared with the control lanes. To gain a more quantitative

(19) Additional evidence for DNA conformational changes was found by atomic force microscopy imaging of DNA fragments in which DNA complexed by **6b** was seen to be more curved than the same but uncomplexed DNA (Hansma, H. G.; Browne, K. A.; Bezanilla, M.; Bruice, T. C. *Biochemistry* Submitted for publication).

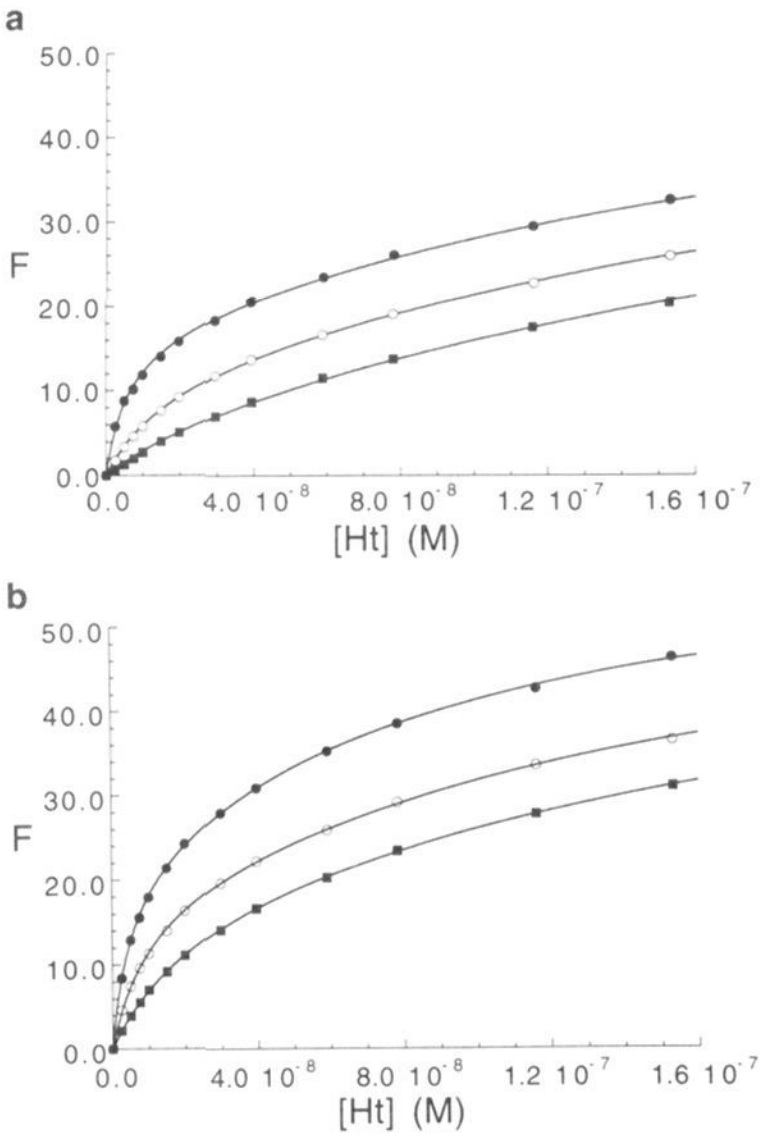

Figure 5. Plot of fluorescence (F, in arbitrary units) vs Hoechst 33258 (**Ht**) concentration at pH 7.0 and 35 °C for (a) **6a** and (b) **6b** at 8.0×10^{-9} M (●), 1.0×10^{-8} M (○), and 1.2×10^{-8} M (■) in the presence of 5.0×10^{-9} M hexadecamer duplex. The theoretical curves which fit the points were computer generated by use of eq 1.

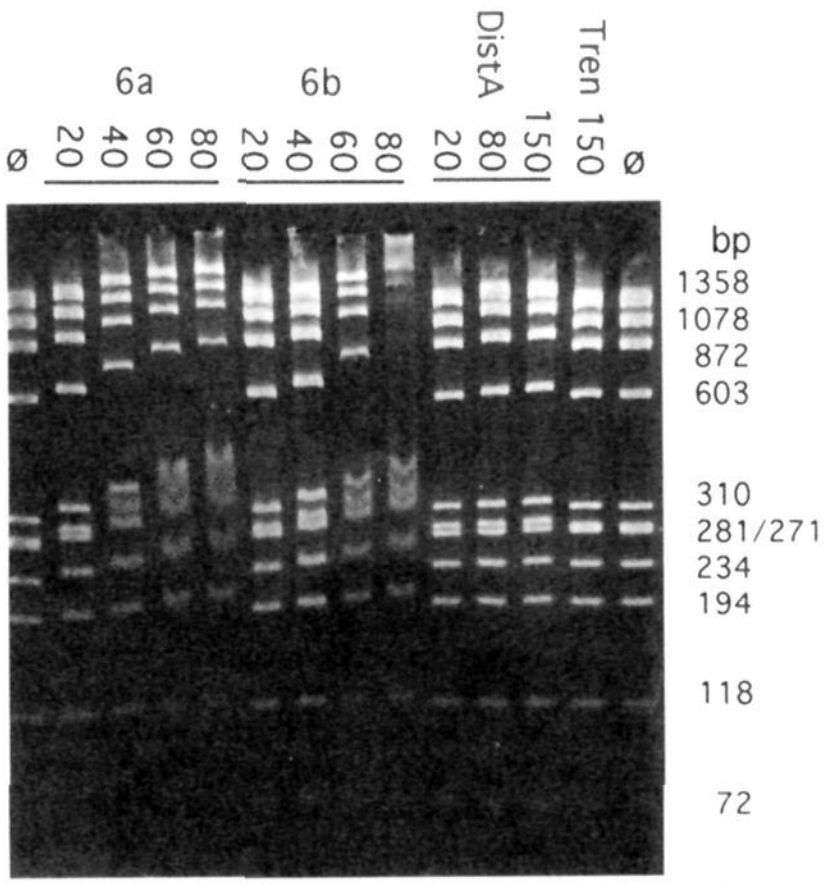

Figure 6. Effect of DNA binding on the electrophoretic mobility of ϕX-174-RF DNA *Hae*III restriction digest fragments (sizes indicated to the right side of the figure). In lanes 1 and 14, ϕ indicates control DNA; lanes 2–13, the indicated concentrations of **6a**, **6b**, distamycin (**DistA**), and tris(2-aminoethyl)amine (Tren) are in μM.

appreciation for the magnitude of the DNA structural changes occuring with the association of the tren-microgonotropens, the migration data has been reduced to a graphical form.

The electrophoretic mobilities of the ϕX-174-RF DNA *Hae*III restriction digest fragments have been calculated as the R_L values when coelectrophoresed with **6a**, **6b**, **Dm**, and tris(2-aminoethyl)-amine. {R_L is the ratio of the apparent length to real length where apparent length is the length of uncomplexed dsDNA (interpolated or slightly extrapolated from the standards) with same mobility.}[20] *The representative plot of R_L vs bp at 80 μM* **6a** and **6b**, or 150 μM distamycin {Figure 7a} shows that as the size of the fragment increases, the effect of these agents is to increase the apparent size of DNA fragments (decrease the mobility) relative to the control (ϕX-174-RF DNA with no added agent). The order of effectiveness in increasing the apparent length of ϕX-174-RF DNA *Hae*III restriction digest fragments is **6a** ~ **6b** ≫ distamycin > tren. The R_L value does not vary as a simple function with increasing DNA fragment size. Instead, variation in migration patterns is probably contingent on the number of A + T-rich sequences in each fragment, the relative

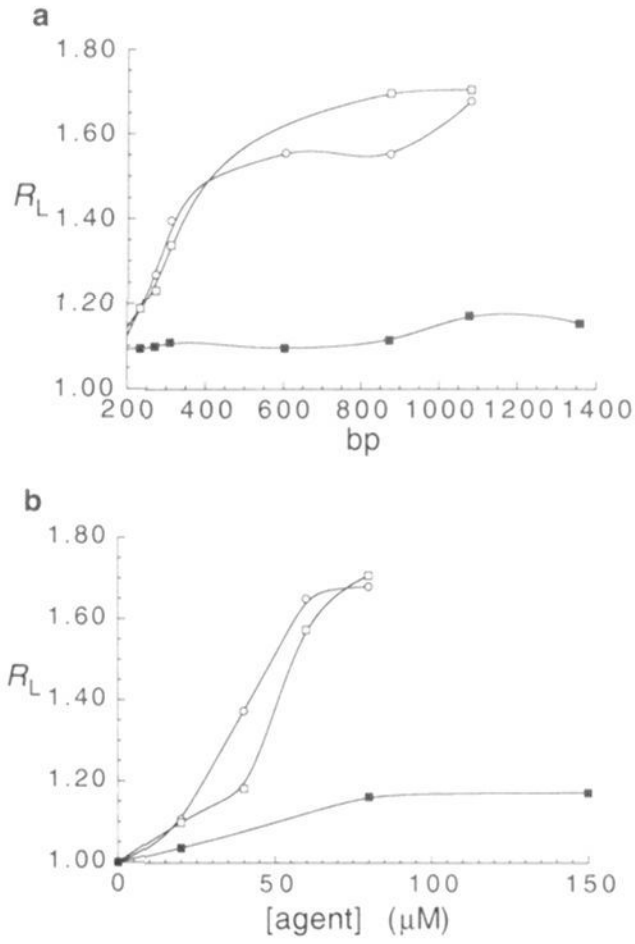

Figure 7. (a) A plot of the ratio of apparent DNA length to real length (R_L) vs the number of base pairs (bp) in the longest and intermediate sized DNA fragments in the presence of 80 μM **6a** (○) or **6b** (□) and 150 μM distamycin (■). (b) R_L vs agent concentration, [agent], {**6a** (○), **6b** (□), and distamycin (■)} when examining the 1078 bp DNA fragment. The curves are interpolations between the data points for **6a**, **6b**, and distamycin. The data for parts a and b were generated from Figure 6 *as explained in the text.*

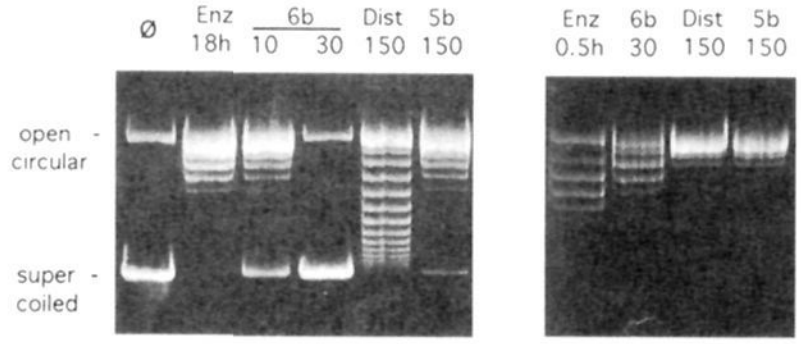

Figure 8. The effect of **6b**, distamycin, and **5b**[4] on the ability of calf thymus topoisomerase I to relax 1 μg of supercoiled pBR322 at 37 °C. The lanes are labeled with the name and the μM concentration of the reagent used. In the first panel, the pBR322 was preincubated with or without **6b**, distamycin, or **5b** for 60 min before the 18-h incubation with toposiomerase I (except for the (–) control, ϕ). In the second panel, pBR322 was incubated with toposiomerase I for 30 min before the addition of **6b**, distamycin, or **5b** and the subsequent 18-h incubation.

(20) Wu, H.-M.; Crothers, D. M. *Nature* **1984**, *308*, 509.

Table 1. Mean Values of the Association and Quenching Constants for Ht, **Dm**, **2**, **5a**, **5b**, **5c**, and the New Ligands **6a** and **6b** to d(GGCGCAAATTTGGCGG)/d(CCGCCAAATTTGCGCC) {in H_2O, 10 mM Phosphate Buffer, pH 7.0, and 10 mM NaCl at 35 °C}

ligand	log K_{L1}	log K_{L2}	log $K_{L1}K_{L2}$	log K_{HtL}	log K_{LHt}	Q'
Ht[a,b]	7.6 ± 0.1	9.1 ± 0.2				
Dm[a,c]	7.6 ± 0.09	8.4 ± 0.08	16.0	8.8 ± 0.09	8.8	
2[a,d]	6.8 ± 0.1	6.2 ± 0.5	13.0	−1.2 ± 0.1	−1.3	
5a[a,c]	8.5 ± 0.3	8.9 ± 0.02	17.4	10.0 ± 0.07	8.9	0.53 ± 0.20
5b[a,c]	8.3 ± 0.2	8.8 ± 0.2	17.1	10.0 ± 0.06	9.2	0.57 ± 0.064
5c[a,c]	8.2 ± 0.2	8.8 ± 0.05	17.0	9.9 ± 0.02	9.2	0.55 ± 0.081
6a[e]	9.2 ± 0.1	9.2 ± 0.1	18.4	10.7 ± 0.01	8.8	0.41 ± 0.11
6b[e]	8.9 ± 0.08	9.0 ± 0.2	17.9	10.3 ± 0.1	8.8	0.64 ± 0.046

[a] A recalculation of previously determined association constants[5] with the curve fitting program SigmaPlot (Jandel Scientific). [b] The constants were calculated from the mean values of three titration experiments of the hexadecamer with Ht. The standard deviations are σ_n. [c] The standard deviations, σ_n, are from the mean values of the constants calculated at 8.0×10^{-9}, 1.0×10^{-8}, 1.2×10^{-8}, and 1.4×10^{-8} M ligand. [d] The standard deviations, σ_n, are from the mean values of the constants calculated at 5.0×10^{-8} and 1.0×10^{-7} M **2**. [e] The standard deviations, σ_n, are from the mean values of the constants from two experiments calculated at 8.0×10^{-9}, 1.0×10^{-8}, and 1.2×10^{-8} M in **6a** or **6b**.

positions of the A + T-rich sequences within a given fragment,[21] and the porosity of the gel.[22] In addition, the plot of R_L vs [agent] for the 1078 bp fragment in Figure 7b shows that tren-microgonotropen-a and -b's influence on the DNA conformation is quite concentration dependent and sigmoidal in response. Distamycin does not demonstrate very marked changes even at the highest concentrations examined. In fact, the effect of distamycin on these fragments is nearly concentration independent over the concentration ranges examined. As is evident from the above discussion and previous work from this laboratory,[4] tren-microgonotropens are about twice as effective in inducing structural changes in DNA as are the dien-microgonotropens (nearly the same decrease in electrophoretic mobility is seen for **6a**, **b** at ca. half of the concentration that was used for **5a–c**) and at least four times as effective in inducing structural changes as in **Dm**.

The fact that the tren-microgonotropens are only ca. twice as effective as the dien-microgonotropens in retarding gel electrophoretic migration of DNA fragments is somewhat surprising considering the fact that the complex equilibrium association constants ($K_{L1}K_{L2}$, Table 1) for **6a** {2×10^{18} M} and **6b** {8×10^{17} M} are considerably higher (4- to 20-fold) than those of the dien-microgonotropens {$1–2 \times 10^{17}$ M}. This suggests that the mode of inhibition of DNA mobility in an electrophoretic field is not simply a function of how tight a ligand binds to the DNA. Instead, the degree of inhibition is likely due to a less tangible quality of the microgonotropen which induces a DNA conformational change upon association.

Topoisomerase I Inhibition by 6b. Mammalian topoisomerase I (topoI) is an enzyme that relaxes both positive and negative superhelical turns in covalently closed circular DNA. It performs this ATP-independent reaction by transiently breaking the phosphodiester linkage of one strand of DNA, passing the intact strand through the break, and then religating the gap. In this manner, the enzyme effectively decreases the superhelical density by changing the linking number of the closed circular DNA in integer values.[23]

Inhibition of topoI's action on supercoiled pBR322 by **6b** was compared to inhibition by **Dm** and **5b** (dien-microgonotropen-b). In the first set of experiments, each agent was allowed to incubate with the DNA for 1 h prior to the 18 h topoI reaction period. The topoI (+) control {Enz, 18 h; Figure 8} shows the extent of superhelical relaxation found in the absence of added **5b**, **6b**, or **Dm**, while the (−) control {ϕ} shows the spontaneous background relaxation. The (+) control amount of relaxation is roughly the same amount seen in the presence of 150 μM **5b** (4.95 molecules of **5b**/bp; essentially no inhibition). With 150 μM **Dm**, a continuous family of topological isomers separated by single linking numbers is generated from supercoiled to completely relaxed circular pBR322 indicating partial inhibition (the number of topological isomers is somewhere between the (+) and the (−) controls). At 10 μM **6b** (0.33 molecules of **6b**/bp) a considerable number of the same topological isomers as for **Dm** at 150 μM can be seen even though the predominent isomer is the fully supercoiled species. By 30 μM **6b** (0.99 molecules of **6b**/bp), complete inhibition of topoI takes place.

In closely related experiments, the mode of inhibition of topoI was examined. This was accomplished by allowing the supercoiled DNA to be partially relaxed for 0.5 h with topoI before any other DNA ligands were added {Figure 8}. The 0.5 h control {Enz, 0.5 h} shows the state of unwinding at the time **5b**, **6b**, and **Dm** were added. While 150 μM **5b** and **Dm** demonstrated no effect (compare with the topoI (+) control), 30 μM **6b** inhibited topoI even after pBR322 was considerably unwound. This indicates that of the three compounds surveyed, only **6b** is able to effectively compete with topoI once the enzyme is bound. Extrapolating from experiments with the hexadecamer d(GGCGCAAATTTGGCGG)/d(CCGCCAAATTTGCGCC) (Table 1), one might anticipate the binding affinity of **6b** to pBR322 to be in the range of 2- to 4-fold greater than the same binding affinity of **5b**, The 2- to 4-fold difference in binding does not explain the inhibition data {Figure 8}. This suggests that, as with the electrophoretic mobility shift assay, binding of **6b** to DNA alters the conformation of DNA, Such an altered DNA conformation could inhibit topoI by either preventing enzyme binding to or "tracking" along DNA or by generating conformationally uncleavable sites.

Experimental Section

Organic Synthesis Materials. Reagent grade chemicals were used without purification unless otherwise stated. Methanol was refluxed and distilled from CaH_2. Dimethylformamide (DMF) was dried by CaH_2 overnight and distilled under reduced pressure. Triethylamine was dried by KOH and distilled. Methanol, DMF, and trimethylamine were stored over 4A molecular sieves. Tetrahydrofuran (THF) was refluxed with Na metal and distilled before use. Tris(2-aminoethyl)amine, diisopropylethylamine, and diethyl cyanophosphonate (DECP) were purchased from Aldrich. 2-(Trimethylsilyl)ethyl *p*-nitrophenyl carbonate and *tert*-butyl *S*-4,6-dimethyl-pyrimid-2-yl thiocarbonate were purchased from Fluka. After treatment with 1 M NaOH, ion-exchange resin (Aldrich) was washed with distilled water and methanol before using. Ethyl 1-(3-propal)-4-nitro-2-pyrrolecarboxylate (**7a**), ethyl 1-(4-butal)-4-nitro-2-pyrrolecarboxylate (**7b**), and dimethyl 3-(1-methyl-4-nitro-2-pyrrolecarboxamido)propionamine (**11**) were synthesized by the methods published in a previous paper of this series.[4] 1-Methyl-4-nitro-2-pyrrolecarbonyl chloride was synthesized from reaction of 1-methyl-4-nitro-2-pyrrolecarboxylic acid, prepared by nitration of 1-methyl-2-pyrrolecarboxylic acid (Aldrich),[24] and thionyl chloride according to the published methods.[24b,25]

(21) Levene, S. D.; Wu, H.-W.; Crothers, D. M. *Biochemistry* **1986**, *25*, 3988.
(22) Thompson, J. F.; Landy, A. *Nucleic Acids Res.* **1988**, *16*, 9687.
(23) Lewin, B. *Genes*, 2nd ed.; John Wiley & Sons: New York, 1985.
(24) (a) Bialer, M.; Yagen, B.; Mechoulam, R. *Tetrahedron* **1978**, *34*, 2389. (b) Lown, J. W.; Krowicki, K. *J. Org. Chem.* **1985**, *50*, 3774. (c) Youngquist, R. S. Ph. D. Dissertation, California Institute of Technology, 1988.
(25) Rao, K. E.; Bathini, Y.; Lown, J. W. *J. Org. Chem.* **1990**, *55*, 728.

General Organic Synthesis Methods. Infrared (IR) spectra were obtained in KBr or neat on a Perkin-Elmer monochromator grating spectrometer (Model 1330). Low-resolution mass spectra (LRMS) were recorded on a VG Analytical spectrometer (Model VGII-250) by fast atom bombardment (FAB) using *m*-nitrobenzyl alcohol (NBA) as a matrix. High-resolution mass spectrometry (HRMS) was performed at the Midwest Center for Mass Spectrometry Laboratory at the University of Nebraska (Lincoln, NE) using FAB technique and NBA matrix. ^{1}H NMR spectra were obtained in $CDCl_3$ or in DMSO-d_6 with a General Electric GN-500 spectrometer. Chemical shifts are reported in δ (ppm) relative to $CHCl_3$ (7.24 ppm) or to DMSO (2.49 ppm) with s, d, t, q, and m signifying singlet, doublet, triplet, quartet, and multiplet; coupling constants (J) are reported in hertz (Hz). Chromatographic silica gel (Fisher Chemical, 200–425 mesh) was used for flash chromatography, and glass-backed plates of 0.25-mm SiO_2 60-F_{254} (Merck) were used for thin-layer chromatography (TLC). All nonaqueous reactions were run under argon with rigorous exclusion of water unless otherwise noted.

(8a). To a solution of tris(2-aminoethyl)amine (5.0 g, 34 mmol) and acetic acid (5.0 g, 83 mmol) in 200 mL of MeOH was added ethyl 1-(3-propal)-4-nitro-2-pyrrolecarboxylate (**7a**) (1.3 g, 5.4 mmol) in 100 mL of MeOH dropwise over 30 min at 0 °C followed by $NaCNBH_3$ (0.6 g, 10 mmol). After addition the solution was stirred at room temperature for 72 h. The reaction was followed by TLC (SiO_2, hexane:EtOAc = 3:1). After complete disappearance of **7a**, the solution was concentrated, and the residue obtained was dissolved in 300 mL of CH_2Cl_2. The CH_2Cl_2 solution was washed with 50 mL of 1 N aqueous NaOH and dried over K_2CO_3. Removal of the solvent gave crude **8a** which contained <5% impurity as shown by ^{1}H NMR, and **8a** thus obtained was used in the next reaction without further purification. **8a**: 1.7 g, 85%; pale yellow oil; ^{1}H NMR ($CDCl_3$) δ 1.34 (t, J = 7, –COOCCH$_3$, 3H), 1.87 (bs, –NH + H_2O), 1.95 (m, –CCH$_2$C–, 2H), 2.49–2.76 (m, –CCH$_2$N–, 14H), 4.28 (q, J = 7, –COOCH$_2$C, 2H), 4.44 (t, J = 7, pyrrole NCH$_2$C–, 2H), 7.41 (d, J = 2, pyrrole Ar–H, 1H), 7.72 (d, J = 2, pyrrole Ar–H, 1H); LRMS (FAB) 371 (M + H$^+$).

(8b). The procedure used for the synthesis of **8b** was much the same as employed for **8a**. **8b**: 3.1 g, 97%; pale yellow oil; ^{1}H NMR (DMSO-d_6) δ 1.28 (t, J = 7, –COOCCH$_3$, 3H), 1.32 – 1.60 (m, –CCH$_2$C–, 2H), 1.65–1.78 (m, –CCH$_2$C–, 2H), 2.38 – 2.60 (m, –CCH$_2$N–, 14H), 3.04 (bs, –NH + H_2O), 4.25 (q, J = 7, –COOCH$_2$C, 2H), 4.34 (t, J = 7, pyrrole NCH$_2$C–, 2H), 7.33 (d, J = 2, pyrrole Ar–H, 1H), 8.32 (d, J = 2, pyrrole Ar–H, 1H); LRMS (FAB) 385 (M + H$^+$).

(9a). A solution of **8a** (1.7 g, 5 mmol), diisopropylethylamine (5 mL), and 2-(trimethylsilyl)ethyl *p*-nitrophenyl carbonate (7.1 g, 25 mmol) in 100 mL of MeOH was stirred at 60 °C for 10 h. TLC (SiO_2, hexane:EtOAc = 1:1) showed complete disappearance of the reactant. After cooling, the solution was concentrated, and the residue obtained was dissolved in 300 mL of CH_2Cl_2. The organic solution was washed with 100 mL of 5% aqueous Na_2CO_3 and 100 mL of saturated aqueous NaCl and dried over Na_2SO_4. Removal of the solvent gave a yellow-oil product mixture which was loaded on SiO_2 column, and elution with a solvent mixture of hexane:EtOAc:Et_3N = 20:10:3 gave pure **9a** as a pale yellow viscous oil. **9a**: 2.1 g, 52%; TLC (SiO_2, hexane:EtOAc:Et_3N = 30:10:3) R_f 0.37; ^{1}H NMR (DMSO-d_6) δ –0.10 (s, –SiCH$_3$, 27H), 0.82–0.90 (m, –CH$_2$Si–, 6H), 1.25 (t, J = 7, –COOCCH$_3$, 3H), 1.85–1.95 (m, –CCH$_2$C–, 2H), 2.39–2.51 (m, –CCH$_2$N–, 6H), 2.94–3.18 (m, –OCONCH$_2$C–, 8H), 3.93–4.00 (m, –NCOOCH$_2$C–, 6H), 4.22 (q, J = 7, –COOCH$_2$C, 2H), 4.30 (bs, pyrrole NCH$_2$C–, 2H), 6.77 (bs, –OCONH–, 2H), 7.28, 8.29 (2s, pyrrole Ar–H, 2H); LRMS (FAB) 803 (M + H$^+$).

(9b). The procedure used for the synthesis of **9b** was much the same as employed for **9a**. **9b**: 4 g, 61%; TLC (SiO_2, hexane:EtOAc:Et_3N = 30:10:3) R_f 0.37; IR (neat): ν_{N-H} = 3300–3500 cm^{-1}, $\nu_{C=O}$ = 1680–1720 cm^{-1}, ν_{N-O} = 1320, 1510 cm^{-1}; ^{1}H NMR (DMSO-d_6) δ –0.11 (s, –SiCH$_3$, 27H), 0.85–0.92 (m, –CH$_2$Si–, 6H), 1.26 (t, J = 7, –COOCCH$_3$, 3H), 1.39–1.43 (m, –CCH$_2$C–, 2H), 1.64–1.67 (m, –CCH$_2$C–, 2H), 2.41–2.51 (m, –CCH$_2$N–, 6H), 2.94–3.17 (m, –OCONCH$_2$C–, 8H), 3.97–4.02 (m, –NCOOCH$_2$C–, 6H), 4.25 (q, J = 7, –COOCH$_2$C, 2H), 4.36 (t, J = 7, pyrrole NCH$_2$C–, 2H), 6.79 (bs, –OCONH–, 2H), 7.31, 8.30 (2s, pyrrole Ar–H, 2H); LRMS (FAB) 817 (M + H$^+$).

(10a). NaOH (0.32 g, 8 mmol) in 20 mL of H_2O was added to a solution of **9a** (2.0 g, 2.5 mmol) in 20 mL of EtOH. The resulting solution was stirred at room temperature for 10 h. Et_3N·HCl (2.2 g, 16 mmol) was added to the solution when TLC (SiO_2, hexane:EtOAc:Et_3N = 20:10:3) showed disappearance of the reactant. The color of the solution turned from orange to pale yellow. The solution was concentrated to dryness under reduced pressure, and the residue was dissolved in 200 mL of CH_2Cl_2. The pale yellow organic phase was washed with 30 mL of H_2O and dried over Na_2SO_4. Removal of the solvent gave the product as a yellow viscous oil. **10a**: 1.6 g, 73%; ^{1}H NMR (DMSO-d_6) δ –0.10 (s, –SiCH$_3$, 27H), 0.86–0.92 (m, –CH$_2$Si–, 6H), 1.13 (t, J = 7, –NCCH$_3$, 9H), 1.89–1.95 (m, –CCH$_2$C–, 2H), 2.40–2.48 (m, –CCH$_2$N–, 6H), 2.94–3.18 (m, –OCONCH$_2$C– + –CH$_2$N$^+$–, 14H), 3.33 (bs, –NH$^+$– + H_2O), 3.97–4.03 (m, –NCOOCH$_2$–, 6H), 4.38 (bs, pyrrole NCH$_2$C–, 2H), 6.86 (bs, –OCONH–, 2H), 7.03, 8.06 (2s, pyrrole Ar–H, 2H); LRMS (FAB) 775 (M – Et_3N + H$^+$).

(10b). The procedure used for the synthesis of **10b** was much the same as employed for **10a**. **10b**: 4 g, 92%; IR (KBr) ν_{N-H} = 3400–3700 cm^{-1}, ν_{N^+-H} = 2600–2900 cm^{-1}, $\nu_{C=O}$ = 1680–1720 cm^{-1}, ν_{N-O} = 1260, 1520 cm^{-1}; ^{1}H NMR (DMSO-d_6) δ –0.10 (s, –SiCH$_3$, 27H), 0.84–0.92 (m, –CH$_2$Si–, 6H), 1.14 (t, J = 7, –NCCH$_3$, 9H), 1.35–1.45 (m, –CCH$_2$C–, 2H), 1.60 – 1.70 (m, –CCH$_2$C–, 2H), 2.40–2.48 (m, –CCH$_2$N–, 6H), 2.95–3.15 (m, –OCONCH$_2$C– + –CH$_2$N$^+$–, 14H), 3.38 (bs, –NH$^+$– + H_2O), 3.97–4.03 (m, –NCOOCH$_2$C–, 6H), 4.43 (t, J = 7, pyrrole NCH$_2$C–, 2H), 6.86 (bs, –OCONH–, 2H), 7.02, 8.03 (2s, pyrrole Ar–H, 2H); LRMS (FAB) 789 (M – Et_3N + H$^+$).

(12a). A solution of **11** (0.46 g, 1.8 mmol) in 100 mL of MeOH was hydrogenated at atmospheric pressure over 10% palladium on charcoal (0.5 g) at room temperature. The catalyst was removed by filtration, and the filtrate was concentrated. To the residue was added **10a** (1.6 g, 1.8 mmol) in dry DMF (100 mL). After cooling to 0 °C, DECP (0.33 g, 2.0 mmol) and Et_3N (1.0 g, 10 mmol) were added dropwise to the solution. The solution was stirred at 0 °C for 2 h and at room temperature for another 10 h. Solvent was evaporated to dryness *in vacuo*, and the resulting residue was dissolved in 400 mL of CH_2Cl_2. The organic phase was washed with 80 mL of 5% aqueous Na_2CO_3 and dried over K_2CO_3. The crude product was purified with a flash column (SiO_2, EtOAc:MeOH:Et_3N = 50:10:3) to give **12a** as a yellow glassy solid. **12a**: 1 g, 64%; TLC (SiO_2, EtOAc:MeOH:Et_3N = 50:10:3) R_f 0.59; ^{1}H NMR (DMSO-d_6) δ –0.17 (s, –SiCH$_3$, 27H), 0.84–0.92 (m, –CH$_2$Si–, 6H), 1.55–1.62 (m, –CONCCH$_2$C–, 2H), 1.92–2.00 (m, –CCH$_2$C–, 2H), 2.12 (s, –NCH$_3$, 6H), 2.23 (t, J = 7, –CH$_2$NMe, 2H), 2.43–2.48 (m, –CCH$_2$N–, 6H), 2.95–3.02 (m, ArCONCH$_2$C–, 2H), 3.12–3.23 (m, –OCONCH$_2$C–, 8H), 3.79 (s, pyrrole N–CH$_3$, 3H), 3.97–4.03 (m, –NCOOCH$_2$C–, 6H), 4.40 (bs, pyrrole NCH$_2$C–, 2H), 6.78 (bs, –OCONH–, 2H), 6.79, 7.19, 7.59, 8.22 (4s, pyrrole Ar–H, 4H); 8.04, 10.21 (2bs, –CONH–, 2H); LRMS (FAB) 981 (M + H$^+$).

(12b). The procedure used for the synthesis of **12b** was much the same as employed for **12a**. **12b**: 2.7 g, 60%; TLC (SiO_2, EtOAc:MeOH:Et_3N = 50:10:3) R_f 0.59; IR (KBr) ν_{N-H} = 3200–3600 cm^{-1}, $\nu_{C=O}$ = 1650–1720 cm^{-1}, ν_{N-O} = 1310, 1520 cm^{-1}; ^{1}H NMR (DMSO-d_6) δ –0.17 (s, –SiCH$_3$, 27H), 0.84–0.92 (m, –CH$_2$Si–, 6H), 1.38–1.45 (m, –CCH$_2$C–, 2H), 1.57–1.64 (m, –CONCCH$_2$C–, 2H), 1.65–1.73 (m, –CCH$_2$C–, 2H), 2.14 (s, –NCH$_3$, 6H), 2.24 (t, J = 7, –CH$_2$NMe, 2H), 2.43–2.47 (m, –CCH$_2$N–, 6H), 2.96–3.00 (m, ArCONCH$_2$C–, 2H), 3.10–3.20 (m, –OCONCH$_2$C–, 8H), 3.79 (s, pyrrole NCH$_3$, 3H), 3.97–4.04 (m, –NCOOCH$_2$C–, 6H), 4.42 (t, J = 7, pyrrole NCH$_2$C–, 2H), 6.79 (bs, –OCONH–, 2H), 6.80, 7.19, 7.58, 8.19 (4s, pyrrole Ar–H, 4H), 8.09, 10.20 (2bs, –CONH–, 2H); LRMS (FAB) 995 (M + H$^+$).

(13a). A solution of **12a** (1.0 g, 1.0 mmol) in 100 mL of DMF was hydrogenated at atmospheric pressure over 10% palladium on charcoal (0.5 g) at 50 °C. The catalyst was removed by filtration, the filtrate was concentrated, and the resulting residue was dissolved in dry DMF (100 mL). After cooling down to 0 °C, 1-methyl-4-nitro-2-pyrrolecarbonyl chloride (0.2 g, 1.1 mmol) and Et_3N (0.3 g, 3 mmol) were added. The solution was stirred at 0 °C for 2 h and at room temperature for another 10 h. The solution was concentrated to dryness *in vacuo*, and the resulting residue was dissolved in 300 mL of CH_2Cl_2. The organic phase was washed with 50 mL of aqueous 5% Na_2CO_3 and dried over K_2CO_3. The crude product was purified with a flash column (SiO_2, EtOAc:MeOH:Et_3N = 50:10:5) to give **13a** as a pale yellow glassy solid. **13a**: 0.6 g, 54%; TLC (SiO_2, EtOAc:MeOH:Et_3N = 50:5:5) R_f 0.33; ^{1}H NMR (DMSO-d_6) δ –0.18 (s, –SiCH$_3$, 27H), 0.84–0.91 (m, –CH$_2$Si–, 6H), 1.56–1.63 (m, –CONCCH$_2$C–, 2H), 1.86–1.92 (m, –CCH$_2$C–, 2H), 2.14 (s, –NCH$_3$, 6H), 2.24 (t, J = 7, –CH$_2$NMe, 2H), 2.43 – 2.48 (m, –CCH$_2$N–, 6H), 2.94–3.00 (m, ArCONCH$_2$C–, 2H), 3.12–3.20 (m, –OCONCH$_2$C–, 8H), 3.79, 3.95 (2s, pyrrole N–CH$_3$, 6H), 3.97–4.04 (m, –NCOOCH$_2$C–, 6H), 4.29 (t, J = 7, pyrrole NCH$_2$C–, 2H), 6.78

(26) Hore, P. J. *J. Magn. Reson.* **1983**, *55*, 283.
(27) Sambrook, J.; Fritsch, E. F.; Maniatis, T. *Molecular Cloning, A Laboratory Manual*; 2nd ed.; Cold Spring Harbor: New York, 1989.

(bs, –OCONH–, 2H), 6.80, 7.01, 7.19, 7.33, 7.59, 8.18 (6s, pyrrole Ar–H, 6H), 8.05, 9.93, 10.28 (3bs, –CONH–, 3H), LRMS (FAB) 1103 (M + H^+).

(13b). The procedure used for the synthesis of **13b** was much the same as employed for **13a**. **13b**: 2 g, 66%; TLC (SiO_2, EtOAc:MeOH:Et_3N = 50:5:5) R_f 0.33; IR (KBr) ν_{N-H} = 3100–3500 cm^{-1}, $\nu_{C=O}$ = 1650–1720 cm^{-1}, ν_{N-O} = 1310, 1520 cm^{-1}; ^1H NMR (DMSO-d_6) δ –0.16 (s, –$SiCH_3$, 27H), 0.85–0.94 (m, –CH_2Si–, 6H), 1.38–1.43 (m, –CCH_2C–, 2H), 1.58–1.63 (m, –$CONCCH_2C$–, 2H), 1.60–1.65 (m, –CCH_2C–, 2H), 2.13 (s, –NCH_3, 6H), 2.24 (t, J = 7, –CH_2NMe, 2H), 2.43–2.48 (m, –CCH_2N–, 6H), 2.95–3.02 (m, $ArCONCH_2C$–, 2H), 3.12–3.20 (m, –$OCONCH_2C$–, 8H), 3.79, 3.95 (2s, pyrrole NCH_3, 6H), 3.97–4.05 (m, –$NCOOCH_2C$–, 6H), 4.31 (t, J = 7, pyrrole NCH_2C–, 2H), 6.78 (bs, –OCONH–, 2H), 6.81, 7.00, 7.18, 7.32, 7.58, 8.18 (6s, pyrrole Ar–H, 6H), 8.06, 9.92, 10.28 (3bs, –CONH–, 3H); LRMS (FAB) 1117 (M + H^+).

(14a). A solution of **13a** (0.6 g, 0.6 mmol) in 100 mL of DMF was hydrogenated at atmospheric pressure over 10% palladium on charcoal (0.5 g) at 60 °C. The catalyst was removed by filtration, the filtrate was concentrated, and the resulting residue was dissolved in dry DMF (100 mL). After cooling down to 0 °C, CH_3COCl (0.08 g, 1.0 mmol) and Et_3N (0.3 g, 3.0 mmol) were added dropwise. The solution was stirred at 0 °C for 2 h and at room temperature for another 10 h. The solution was concentrated to dryness *in vacuo*, and the resulting residue was dissolved in 300 mL of CH_2Cl_2. The organic phase was washed with 50 mL of aqueous 5% Na_2CO_3 and dried over K_2CO_3. The crude product was purified with a flash column (SiO_2, EtOAc:MeOH:Et_3N = 50:20:5) to give **14a** as a pale yellow glassy solid. **14a**: 0.3 g, 45%; TLC (SiO_2, EtOAc:MeOH:Et_3N = 50:20:5) R_f 0.27; ^1H NMR (DMSO-d_6) δ –0.15 (s, –$SiCH_3$, 27H), 0.86–0.90 (m, –CH_2Si–, 6H), 1.58–1.63 (m, –$CONCCH_2C$–, 2H), 1.86–1.92 (m, –CCH_2C–, 2H), 1.96 (s, CH_3CON–, 3H), 2.17 (s, –NCH_3, 6H), 2.28 (t, J = 7, –CH_2NMe, 2H), 2.43–2.48 (m, –CCH_2N–, 6H), 2.94–3.00 (m, $ArCONCH_2C$–, 2H), 3.15–3.22 (m, –$OCONCH_2C$–, 8H), 3.79, 3.82 (2s, pyrrole N–CH_3, 6H), 3.98–4.06 (m, –$NCOOCH_2C$–, 6H), 4.27 (t, J = 7, pyrrole NCH_2C–, 2H), 6.79 (bs, –OCONH–, 2H), 6.81, 6.86, 7.02, 7.14, 7.18, 7.31 (6s, pyrrole ArH, 6H); 8.06, 9.82, 9.88, 9.90 (4bs, –CONH–, 4H); LRMS (FAB) 1115 (M + H^+).

(14b). The procedure used for the synthesis of **14b** was much the same as employed for **14a**, **14b**: 1.5 g, 74%; TLC (SiO_2, EtOAc:MeOH:Et_3N = 50:20:5) R_f 0.27; ^1H NMR (DMSO-d_6) δ –0.13 (s, –$SiCH_3$, 27H), 0.86–0.90 (m, –CH_2Si–, 6H), 1.40–1.48 (m, –CCH_2C–, 2H), 1.58–1.65 (m, –CCH_2C– + –$CONCCH_2C$–, 4H), 1.96 (s, CH_3CON–, 3H), 2.16 (s, –NCH_3, 6H), 2.27 (t, J = 7, –CH_2NMe, 2H), 2.43–2.48 (m, –CCH_2N–, 6H), 2.96–3.00 (m, $ArCONCH_2C$–, 2H), 3.11–3.22 (m, –$OCONCH_2C$–, 8H), 3.79, 3.82 (2s, pyrrole N–CH_3, 6H), 3.98–4.06 (m, –$NCOOCH_2C$–, 6H), 4.29 (t, J = 7, pyrrole NCH_2C–, 2H), 6.79 (bs, –OCONH–, 2H), 6.81, 6.85, 7.00, 7.13, 7.17, 7.28 (6s, pyrrole Ar–H, 6H), 8.05, 9.79, 9.86, 9.88 (4bs, –CONH–, 4H); LRMS (FAB) 1129 (M + H^+).

(6a). Ten milliliters of CF_3COOH was cooled in an ice-bath before slowly being added to a solution of **14a** (0.18 g, 0.15 mmol) in 10 mL of CH_2Cl_2 with stirring at 0 °C. The solution was stirred at 0 °C for 2 h and at room temperature for another 2 h. CF_3COOH and CH_2Cl_2 were removed by evaporation, and the resulting residue was dissolved in 50 mL of MeOH. After addition of 20 g of ion-exchange resin (HO^- form) the mixture was stirred for 30 min at room temperature. The resin was removed by filtration, and the filtrate was concentrated under vacuum to give pure **6a** as a pale yellow glassy solid. **6a**: 0.1 g, 98%; ^1H NMR (DMSO-d_6) δ 1.58–1.63 (m, –$CONCCH_2C$–, 2H), 1.78–1.82 (m, –CCH_2C–, 2H), 1.96 (s, CH_3CON–, 3H), 2.12 (s, –NCH_3, 6H), 2.23 (t, J = 7, –CH_2NMe, 2H), 2.34 (t, J = 7, –CCH_2N, 4H), 2.42–2.46 (m, –CCH_2N–, 6H), 2.54–2.64 (m, –CCH_2N–, 6H), 3.16–3.20 (m, $ArCONCH_2C$–, 2H), 3.25 (bs, –CNH_2 + H_2O), 3.79, 3.82 (2s, pyrrole NCH_3, 6H), 4.32 (t, J = 7, pyrrole NCH_2C–, 2H), 6.82, 6.85, 7.00, 7.14, 7.17, 7.27 (6s, pyrrole Ar–H, 6H), 8.11 (t, J = 5.5, ArCONHC–, 1H), 9.80 (s, –CONH–, 1H), 9.90 (bs, –CONH–, 2H); LRMS (FAB) 683 (M + H^+); HRMS (FAB) 683.4467 (calcd for $C_{33}H_{55}N_{12}O_4$ (M+H^+) 683.4469).

(6b). The procedure used for the synthesis of **6b** was much the same as employed for **6a**. **6b**: 0.65 g, 96%; ^1H NMR (DMSO-d_6) δ 1.33–1.40 (m, –CCH_2C–, 2H), 1.56–1.64 (m, –$CONCCH_2C$–, 2H), 1.64–1.71 (m, –CCH_2C–, 2H), 1.96 (s, CH_3CON–, 3H), 2.13 (s, –NCH_3, 6H), 2.23 (t, J = 7, –CH_2NMe, 2H), 2.38 (t, J = 7, –CCH_2N, 4H), 2.42–2.46 (m, –CCH_2N–, 6H), 2.54–2.64 (m, –CCH_2N–, 6H), 3.15–3.20 (m, $ArCONCH_2C$–, 2H), 3.22 (bs, –CNH_2 + H_2O), 3.79, 3.82 (2s, pyrrole NCH_3, 6H), 4.28 (t, J = 7, pyrrole NCH_2C–, 2H), 6.81, 6.86, 7.00, 7.14, 7.17, 7.28 (6s, pyrrole Ar-H, 6H); 8.08 (t, J = 5.5, ArCONHC–, 1H), 9.82, 9.89, 9.92 (3s, –CONH–, 3H); LRMS (FAB) 697 (M + H^+); HRMS (FAB) 697.4631 (calcd for $C_{34}H_{57}N_{12}O_4$ (M + H^+) 697.4625).

Reagents and methods for DNA binding studies were exactly the same as used previously[4,5] unless stated otherwise. The values for the equilibrium constants for **2**, **5a–c**, **Dm**, and Ht were recalculated from previously collected data[5] using the curve fitting program SigmaPlot 4.1.4 (Jandel Scientific, San Rafael, CA). The equilibrium constants for **6a** and **6b** were calculated with SigmaPlot 4.1.4 using the reevaluated constants for **Ht** (K_{Ht1} and K_{Ht2}) and $\sum\Phi \sim 63$. Due to the increased affinity of **6a** for d(GGCGCAAATTTGGCGG)/d(CCGCCAAATTTGCGCC), three additional **Ht** titration points ranging up to 5.5 × 10^{-7} M were required to yield a good computer generated fit.

^1H NMR titrations of 3.8 × 10^{-4} M of the dodecameric duplex d(CGCAAATTTGCG)$_2$ and the hexadecameric duplex d(GGCGCAAATTTGGCGG)/d(CCGCCAAATTTGCGCC) with Hoechst 33258 (**Ht**) were carried out on a GN-500 MHz spectrometer in 0.4 mL of D_2O or in 9:1 H_2O:D_2O (**1-3-3-1** pulse sequence)[26] at 21 °C (0.01 M K_2HPO_4-HCl, pH 7.0, 0.01 M NaCl) unless otherwise specified. The annealing process was as described previously.[5,6] The concentrations of the oligomers were determined in H_2O based on the single-stranded absorbances at 60 °C for the dodecamer (ϵ_{260} = 1.36 × 10^5 M^{-1} cm^{-1}) and at 80 °C for the hexadecamer (ϵ_{260} = 1.72 × 10^5 M^{-1} cm^{-1}). The Ht stock solution (0.01 M) was kept at 2 °C throughout the experiment. All titrant volumes were measured with Hamilton microsyringes. The concentrations of the oligomers and Ht were checked (^1H NMR) before the titration experiment using mesitoate as an internal standard in a 1:1 mol ratio with each compound separately and using an interpulse delay of 10 s. The ^1H NMR integrations were calculated at the 2:1 ratio of Ht/oligomer at 35 °C. The integrations of the ^1H NMR peak areas were consistent with the calculated and the spectrophotometrically determined concentrations.

Topoisomerase I Inhibition Assays. The buffer for all of the 50 μL reactions was composed of 50 mM Tris-HCl, pH 7.5, 50 mM KCl, 10 mM $MgCl_2$, and 1 mM EDTA that was filtered through a sterile 0.45 μ Gelman Sciences Acrodisc. Every reaction mixture contained 1 μg of supercoiled pBR322 plasmid (Pharmacia) and, except for the supercoiled control, every reaction mixture included 20 units of calf thymus topoisomerase I (Bethesda Research Laboratories). For the supercoil relaxation assays, no added agent, 10 or 30 μM **6b**, or 150 μM distamycin (**Dm**), or dien-microgonotropen-b (**5b**)[4] were preincubated with the supercoiled DNA for 60 min before topoisomerase I was added. These reactions were allowed to run for 18 h at 37 °C at which time the reactions were stopped with the addition of 2 μL of 250 mM EDTA, pH 7.5. For the supercoil partial relaxation assays, topoisomerase I was incubated with the supercoiled DNA for 30 min at 37 °C before the addition of 30 μM **6b**, or 150 μM **Dm** or **5b**. These reactions were allowed to run for an additional 18 h at 37 °C after which time they were stopped as described above. The supercoil partial relaxation control was stopped after the initial 30 min at 37 °C. All reactions were extracted twice with water-saturated phenol, extracted once with chloroform, and precipitated with ammonium acetate and ethanol. After the DNA pellets were dissolved in 9 μL of 10 mM Tris-HCl, pH 8.0, and 1 mM EDTA, 1.0 μL of loading buffer[27] {10% (w/v) glycerol, 0.1% (w/v) sodium dodecyl sulfate, and 0.1% (w/v) bromophenol blue} was added to each sample. The different helical forms of pBR322 created by the relaxation assays were electrophoretically separated through a 4% NuSieve 3:1 (hydroxyethylated) agarose gel (vertical, 0.8 mm) in 40 mM Tris-acetate, pH 8.0 and 1 mM EDTA for 8 h at 2 V/cm. The gel was stained with a 0.5 μg/mL solution of ethidium bromide in deionized water for 30 min, destained for 15 min in deionized water, and photographed on a UV (302 nm) transilluminator with Polaroid type 667 film.

Acknowledgment. We express appreciation to the Office of Naval Research and the National Science Foundation for supporting this work. We thank Professor John Carbon for the use of his laboratory facilities in conducting biochemical assays and for his helpful comments. In addition, we gratefully acknowledge the services of J. C. Groppe for assistance in preparation of the molecular biology materials.